Contribution from the Department of Chemistry,
Boston College, Chestnut Hill, Massachusetts 02167

Electrochemical and Spectroelectrochemical Investigations of $[Rh(py)_4Cl_2]Cl$ in Nonaqueous Solvents. Generation and Reactions of Monomeric Rhodium(II) Species

J. E. Anderson* and T. P. Gregory

Received February 1, 1989

An electrochemical and spectroelectrochemical investigation of *trans*-$[Rh(py)_4Cl_2]Cl$ is reported, and the electron-transfer properties of the title complex in acetonitrile, acetonitrile/pyridine, and pyridine solvent systems in the presence and absence of chloride are presented. In the absence of water and oxygen, $[Rh(py)_4Cl_2]Cl$ is reduced by one electron to form either monomeric or dimeric rhodium(II) species, depending upon the solution conditions. In excess pyridine and chloride, a reversible one-electron process is found at $E_{1/2} = -0.74$ V vs SCE, and on the basis of ESR spectroscopy and electrochemical data, formation of $Rh(py)_4Cl_2$ is assigned. The effect of the presence of water on the electron-transfer mechanism will be discussed. In addition, preliminary reaction data of the reduced species with methyl iodide is also presented. From the electrochemical, spectroelectrochemical, and ESR data, a self-consistent electron-transfer mechanism for the reduction of *trans*-$[Rh(py)_4Cl_2]Cl$ is presented.

Recent reports have demonstrated both unusual and fundamental organometallic reactions by the monomeric rhodium(II) complex (P)Rh, where P represents the dianion of a porphyrin macrocycle.[1-8] An important aspect of these studies is the inaccessibility of the rhodium(I) state when the metal is tetracoordinated to this ligand. Electrochemical studies of $\{(P)Rh[NH(CH_3)_2]\}^+$, for example, have demonstrated that, up to potentials of −2.0 V vs SCE in THF, reduction to rhodium(II) and reduction of the porphyrin ring are the only electron-transfer processes.[5] However, the chemical reactions of (P)Rh are limited by the porphyrin macrocycle. Hence, it is of interest to determine if coordination to other nitrogen heterocyclic ligand sets will also prevent observation of rhodium(I) complexes while allowing generation of reactive rhodium(II) species. Studies of $[Rh(bpy)_2Cl_2]^+$ suggest the rhodium(II) state is observable but that rhodium(I) and rhodium(0) complexes are the final reduction products.[9-11] Catalytic reduction of carbon dioxide in the presence of reduced $[Rh(bpy)_2Cl_2]^+$ has also been reported.[12]

We wish to report an electrochemical and spectroelectrochemical investigation of *trans*-$[Rh(py)_4Cl_2]Cl$, where coordination to the four pyridines gives a flexible and neutral N_4 ligand environment. The electron-transfer properties were recorded in acetonitrile, acetonitrile/pyridine, and pyridine solvent systems in the presence and absence of chloride. As will be demonstrated, in the absence of water and oxygen $[Rh(py)_4Cl_2]Cl$ is reduced by one electron to form either monomeric or dimeric rhodium(II) species, depending upon the solution conditions. On the basis of ESR spectroscopy and electrochemical data, one monomeric species is assigned as $Rh(py)_4Cl_2$. Preliminary reaction data following reduction will also be presented and compared with those found for (P)Rh. From the electrochemical, spectroelectrochemical, and ESR data, a self-consistent electron-transfer mechanism for the reduction of *trans*-$[Rh(py)_4Cl_2]Cl$ is presented.

$[Rh(py)_4Cl_2]Cl$ is of interest from several viewpoints, and the synthesis, substitution reactions, and properties have all been investigated,[13-16] including reports of biological activity[17] suggesting potential use as a chemotherapy agent. Of additional interest are the properties, reactions, and reaction mechanisms of rhodium–pyridine-based catalytic systems.[1,16] Electrochemical studies have been performed on $[Rh(py)_4Cl_2]Cl$[16,18-22] in aqueous solvent systems, and the results differ significantly from the data presented in this paper. As will be demonstrated, the differences are probably due to the choice of solvent system.

Experimental Section

Materials. All reagents for synthesis were purchased at the highest level of purity available and were used without purification. For electroanalysis, spectroscopic grade acetonitrile and pyridine were purchased (Aldrich), purified by standard techniques,[23] stored over calcium hydride under an inert atmosphere, and distilled just prior to use. Tetrabutylammonium perchlorate (TBAP) was purchased from Fluka, twice recrystallized from ethanol, and dried in a vacuum oven at 50 °C. Tetrabutylammonium chloride [(TBA)Cl] was purchased from Aldrich and recrystallized three times from methylene chloride under an inert atmosphere by Schlenk techniques. The salt was vacuum-dried, stored under argon, and analyzed by ^1H NMR spectroscopy to check for purity. No signal due to water was found in the ^1H NMR spectrum of the purified salt.

$[Rh(py)_4Cl_2]Cl\cdot 5H_2O$ was synthesized from $RhCl_3\cdot xH_2O$ by methods reported in the literature[13-15] and was obtained in high yield, typically greater than 80%. The UV–visible and IR spectra are in agreement with data published in the literature.[13-15,24] Elemental analysis (Robertson Laboratory) gave the following results: C, 38.48; H, 4.96; N, 8.95. Calcd for $[Rh(py)_4Cl_2]Cl\cdot 5H_2O$: C, 39.00; H, 4.88; N, 9.10.

$[Rh(py)_4Cl_2]Cl$ was reported to lose a pyridine molecule and form $Rh(py)_3Cl_3$ in pyridine,[15] but there is no evidence for this reaction under our solution conditions. Conductivity data suggest a 1:1 electrolyte for solutions of $[Rh(py)_4Cl_2]Cl$ in pyridine, using TBAP as a standard. In addition, ^1H NMR data in pyridine-d_5 and acetonitrile-d_3 are nearly identical, suggesting the presence of the same species under both conditions. In pyridine-d_5, the ^1H NMR data are characterized by a multiplet at 8.65 ppm, a multiplet at 8.02 ppm, and a multiplet at 7.45 ppm. In acetonitrile-d_3, the same basic pattern is observed. There is a multiplet at 8.42 ppm, a multiplet at 8.07 ppm, and a multiplet at 7.45 ppm. Integration of the peaks gives 2:1:2 for the relative number of hydrogens respectively in both solvents. A peak due to water at 5.08 ppm in ace-

(1) Hughes, R. P. In *Comprehensive Organometallic Chemistry*; Wilkinson, G., Ed.; Pergamon Press: New York, 1982; Vol. 5, p 277.
(2) Wayland, B. B.; Woods, B. A.; Coffin, V. L. *Organometallics* **1986**, *5*, 1059.
(3) Del Rossi, K. J.; Wayland, B. B. *J. Am. Chem. Soc.* **1985**, *107*, 7941.
(4) Paonessa, R. S.; Thomas, N. C.; Halpern, J. *J. Am. Chem. Soc.* **1985**, *107*, 4333.
(5) Kadish, K. M.; Yao, C.-L.; Anderson, J. E.; Cocolios, P. *Inorg. Chem.* **1985**, *24*, 4515.
(6) Anderson, J. E.; Yao, C.-L.; Kadish, K. M. *J. Am. Chem. Soc.* **1987**, *109*, 1106.
(7) Anderson, J. E.; Yao, C.-L.; Kadish, K. M. *Organometallics* **1987**, *6*, 706.
(8) Aoyama, Y.; Yoshida, T.; Sakurai, K.-I.; Ogoshi, H. *Organometallics* **1986**, *5*, 168.
(9) Creutz, C.; Kellar, A. D.; Sutin, N.; Zipp, A. P. *J. Am. Chem. Soc.* **1982**, *104*, 3618.
(10) Kew, G.; Hanck, K.; DeArmond, K. *J. Phys. Chem.* **1975**, *79*, 1828.
(11) Kew, G.; DeArmond, K.; Hanck, K. *J. Phys. Chem.* **1974**, *78*, 727.
(12) Bolinger, C. M.; Story, N.; Sullivan, B. P.; Meyer, J. J. *Inorg. Chem.* **1988**, *27*, 4583.
(13) Gillard, R. D.; Osborn, J. A.; Wilkinson, G. *J. Chem. Soc.* **1965**, 1951.
(14) Gillard, R. D.; Heaton, B. T. *J. Chem. Soc. A* **1969**, 451.
(15) Gillard, R. D.; Wilkinson, G. *J. Chem. Soc.* **1964**, 1224.
(16) Jardine, F. H.; Sheridan, P. S. In *Comprehensive Coordination Chemistry*; Wilkinson, G., Ed.; Pergamon Press: New York, 1987; Vol. 4, p 901.
(17) Broomfield, R. J.; Dainty, R. H.; Gillard, R. D.; Heaton, B. J. *Nature* **1969**, *223*, 735.
(18) Willis, J. B. *J. Am. Chem. Soc.* **1944**, *66*, 1067.
(19) Repin, J. A. *J. Appl. Chem. USSR (Engl. Transl.)* **1947**, *20*, 46.
(20) Pantani, F. *J. Electroanal. Chem.* **1963**, *5*, 40.
(21) Addison, A. W.; Gillard, R. D.; Vaughan, D. H. *J. Chem. Soc., Dalton Trans.* **1973**, 1187.
(22) Johnston, L. E.; Page, J. A. *Can. J. Chem.* **1969**, *47*, 2123.
(23) Gordon, A. J.; Ford, R. A. *The Chemist's Companion*; Wiley Interscience: New York, 1972; p 408.
(24) DeArmond, M. K.; Hillis, J. E. *J. Chem. Phys.* **1971**, *54*, 2247.

0020-1669/89/1328-3905$01.50/0

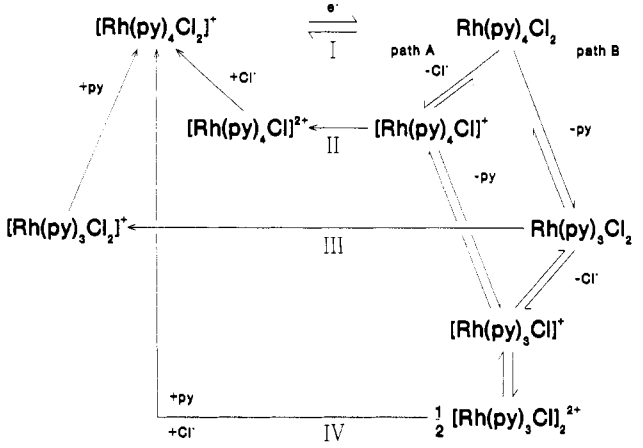

Figure 1. Electron-transfer mechanism for the reduction of $[Rh(py)_4Cl_2]Cl$.

tonitrile and at 2.28 ppm in pyridine is observed. After vacuum-drying, integration gives four water molecules per four molecules of pyridine. Unless otherwise noted, all electrochemical experiments were performed by using vacuum-dried samples of $[Rh(py)_4Cl_2]Cl$.

Equipment and Techniques. Electrochemical experiments were performed on either a BAS-100A or a BAS CV-27 instrument coupled with an EG&G Princeton Applied Research Model RE0091 X-Y Recorder. A platinum-button working electrode, approximate area 0.008 cm^2, a platinum-wire counter electrode, and an SCE reference electrode separated from the solution with a bridge comprised the three-electrode system. All potentials were measured vs the SCE electrode and vs the ferrocene/ferrocenium couple as an internal standard. The supporting electrolyte was 0.1 M TBAP, unless otherwise stated. Low-temperature data were recorded by cooling the cell with a dry-ice acetone bath, monitored with a thermometer. Spectroelectrochemical data were recorded on a Perkin-Elmer Lambda 3B UV–visible spectrophotometer by using one of the above mentioned electrochemical instruments. The electrodes used were a large platinum-working minigrid electrode, a platinum-wire counter electrode, and either an Ag/AgCl reference electrode separated from the solution with a bridge or a wire pseudoreference electrode. The supporting electrolyte was 0.2 M TBAP, unless otherwise stated. The electrochemical cells are home built and are designed for inert-atmosphere studies.

UV–visible spectra were recorded on a Perkin-Elmer Lambda 3B spectrometer, IR spectra were recorded on a Nicolet 510 FT-IR spectrometer, and NMR spectra were recorded on a Varian XL 300-MHz NMR spectrometer. ESR experiments were performed by conventional methods,[25,26] and the spectra were recorded on an IBM Model ED-100 electron spin resonance system. The sample was electrochemically generated under an inert atmosphere, transferred to an ESR cell via Schlenk techniques, and then immediately frozen and stored in liquid nitrogen until measurement. Conductivity experiments were performed on a YSI Model 31A conductivity bridge.

Results and Discussion

Electron-Transfer Mechanism. Electrochemical and spectroelectrochemical studies in acetonitrile, acetonitrile/pyridine, and pyridine in the presence and absence of chloride demonstrate that $[Rh(py)_4Cl_2]Cl$ undergoes a reversible one-electron reduction followed by a series of chemical reactions. The electron-transfer mechanism is summarized in Figure 1 and is supported by the following data.

Figure 2a shows the cyclic voltammogram obtained for a 1.35×10^{-3} M solution of $[Rh(py)_4Cl_2]Cl$ in a 6:1 acetonitrile/pyridine solvent system in the presence of 0.16 M TBAP and 0.06 M (TBA)Cl. In the absence of oxygen, only a one-electron transfer process is found up to −2.0 V vs SCE and is labeled wave 1 (wave 1a, reduction; wave 1b, oxidation) in Figure 2a. Wave 1 has reversible cyclic voltammetric behavior and is a diffusion-controlled one-electron transfer at $E_{1/2} = -0.74 \pm 0.01$ V vs SCE. For wave 1, ΔE_p is 110 mV at a scan rate of 100 mV/s, and the ratio of peak currents is near unity. In addition, the value $E_p - E_{p/2}$ for both waves is 59 mV at this scan rate, and the ratio of the peak current to the square root of the scan rate ($i_p/v^{1/2}$) is a constant.

The same basic electrochemical processes are found at −35 °C as are observed at room temperature, although under these conditions the values of $E_p - E_{p/2}$ and ΔE_p are slightly larger. Differential pulse voltammetry indicates reversible behavior, and bulk electrolysis gives a value of n of 1.0 ± 0.1 upon reduction at −1.20 V. Similar cyclic voltammetric results are obtained when pure pyridine is used as the solvent system. This electron-transfer reaction corresponds to process I in Figure 1.

Figure 3 shows the frozen-solution ESR spectrum of the species generated upon reduction of $[Rh(py)_4Cl_2]Cl$ at −1.00 V vs SCE in pyridine, 0.1 M (TBA)Cl. The spectrum was recorded at −140 °C and is characterized by a $g_\perp$ of 2.28 ± 0.01 and a $g_\parallel$ of 2.00 ± 0.01, indicating a species with axial symmetry. The signal observed for $g_\parallel$ is an eight-line pattern with a value for a of (2.4 ± 0.1) × 10^{-3} cm^{-1}. The relative intensities of the lines are indicated on Figure 3. The number and the relative intensities of the lines can be fit by coupling to one Rh ($I = {}^1/_2$) and two

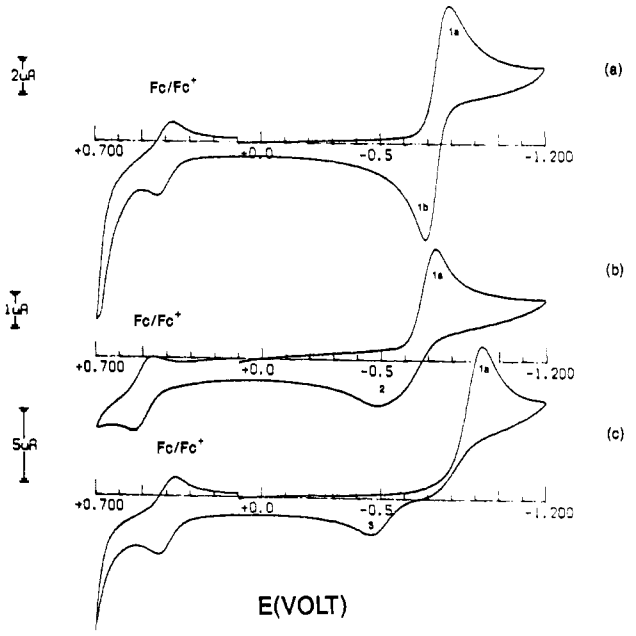

Figure 2. Cyclic voltammograms of $[Rh(py)_4Cl_2]Cl$: (a) 6:1 acetonitrile/pyridine, 0.16 M TBAP and 0.06 M (TBA)Cl, 1.35×10^{-3} M complex, $E_{1/2}$ of ferrocene 0.40 V; (b) pyridine, 0.20 M TBAP, 1.11×10^{-3} M complex, $E_{1/2}$ of ferrocene 0.49 V; (c) acetonitrile, 0.16 M TBAP and 0.06 M (TBA)Cl, 1.35×10^{-3} M complex, $E_{1/2}$ of ferrocene 0.40 V. The ferrocene/ferrocenium couple is also shown.

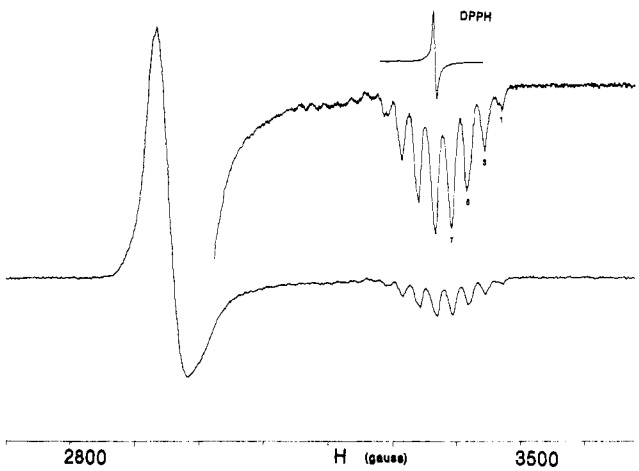

Figure 3. ESR spectrum of a frozen solution of a 2.2×10^{-3} M solution of $[Rh(py)_4Cl_2]Cl$ in 0.1 M (TBA)Cl, pyridine after electrolysis at −1.0 V vs SCE, −140 °C. The relative intensities of $g_\parallel$ are 1:3:5:7:7:5:3:1.

(25) Anderson, J. E.; Liu, Y. H.; Guilard, R.; Barbe, J. M.; Kadish, K. M. *Inorg. Chem.* **1986**, *25*, 2250.
(26) Anderson, J. E.; Liu, Y. H.; Guilard, R.; Barbe, J. M.; Kadish, K. M. *Inorg. Chem.* **1986**, *25*, 3786.

Cl's ($I = {}^3/_2$), where a_{Rh} is equal to a_{Cl}. The outermost lines of $g_\parallel$ could be interpreted as overlapping doublets, but the resolution of the spectrum does not allow for a clear determination. If this were the case, then a_{Rh} would be approximately the same as but not equal to a_{Cl}. Coupling with two Cl's and one Rh agrees with the assignment of Rh(py)$_4$Cl$_2$ as the electrogenerated species under these conditions. The ESR data are also consistent with the addition of the electron to a molecular orbital based on the rhodium d_{z^2} orbital, since coupling to nitrogen is apparently not observed.

Reversible cyclic voltammetric behavior is not found for [Rh(py)$_4$Cl$_2$]$^+$ in the absence of *either* excess pyridine or chloride. This is shown in Figure 2b,c, which contains the cyclic voltammograms of [Rh(py)$_4$Cl$_2$]Cl in pyridine with 0.20 M TBAP (Figure 2b) and in acetonitrile, 0.16 M TBAP and 0.06 M (TBA)Cl (Figure 2c) at a scan rate of 100 mV/s. These results are typical for scan rates of 10–1000 mV/s. The reduction wave (wave 1a, Figure 2b,c) is a diffusion-controlled, reversible one-electron transfer and occurs at $E_{pc} = -0.73 \pm 0.01$ V in pyridine, 0.20 M TBAP (Figure 2b) and at $E_{pc} = -0.93 \pm 0.01$ V in acetonitrile, 0.16 M TBAP and 0.06 M (TBA)Cl (Figure 2c). In each case the reduction process has a value of $E_{pc} - E_{pc/2}$ near 70 mV at 100 mV/s and $i_p/v^{1/2}$ is a constant. In agreement, bulk electrolysis data give values of n of 1.0 ± 0.1 electron for the systems described in Figure 2b,c.

The location of the return processes in Figure 2b,c demonstrates the irreversible behavior and indicates that new species are being reoxidized under the different solvent conditions. The return waves are characterized by $E_{pa} - E_{pa/2} > 80$ mV and in general are not well-defined. However, in pyridine (Figure 2b) the return wave is at $E_{pa} = -0.50 \pm 0.01$ V (wave 2); in the presence of 0.06 M chloride (Figure 2c) the return wave is at $E_{pa} = -0.46 \pm 0.01$ V (wave 3) at a scan rate of 100 mV/s. In addition, a dependence of E_{pa} on the concentration of pyridine for wave 2 and on the concentration of chloride for wave 3 is observed. Cyclic voltammetric results similar to those shown in Figure 2b,c are obtained at −35 °C.

The electrochemical behavior suggests that, following reduction, Rh(py)$_4$Cl$_2$ reacts chemically, and the electron-transfer mechanism is classified as an EC process. In the presence of both pyridine and chloride, the kinetics of the forward chemical reactions are relatively slow and result in reversible cyclic voltammetric behavior. In the absence of either excess pyridine or chloride, even at reduced temperatures, the forward chemical reactions are faster and result in irreversible cyclic voltammetric behavior.

In addition, since both pyridine and chloride are necessary for reversible cyclic voltammetric behavior, two distinct reaction paths must be present, as shown in Figure 1. Either loss of chloride followed by loss of pyridine (path A, Figure 1) or loss of pyridine followed by loss of chloride (path B, Figure 1) occurs after reduction of [Rh(py)$_4$Cl$_2$]Cl. Titration experiments on solutions of [Rh(py)$_4$(Cl)$_2$]$^+$ in acetonitrile, TBAP demonstrate that wave 1a shifts by −63 ± 5 mV per 10-fold change in the concentration of (TBA)Cl, which means that one chloride is lost following reduction. However, no dependence was found for the peak potential of wave 1a on the concentration of pyridine by similar titration experiments. Hence, following reduction, the primary chemical reaction path involves a loss of one chloride to form [Rh(py)$_4$Cl]$^+$ (path A, Figure 1). This implies loss of pyridine following reduction to generate Rh(py)$_3$Cl$_2$ (path B, Figure 1) occurs only in the presence of large concentrations of (TBA)Cl.

Wave 2 is assigned to the reoxidation of [Rh(py)$_4$Cl]$^+$, or process II in Figure 1, on the basis of the cyclic voltammetric behavior. In the presence of excess pyridine, [Rh(py)$_4$Cl]$^+$ would be the predominant species at the electrode surface. By similar reasoning, wave 3 is assigned to reoxidation of Rh(py)$_3$Cl$_2$, since in the presence of excess chloride it would be the predominant species at the electrode surface. This corresponds to process III in Figure 1. ESR experiments on [Rh(py)$_4$Cl$_2$]$^+$ in pyridine, 0.2 M TBAP are in general agreement with this assignment. Under these conditions, a weak signal identical with that shown in Figure 3 is observed, suggesting a faster reaction rate than what is observed when both chloride and pyridine are present.

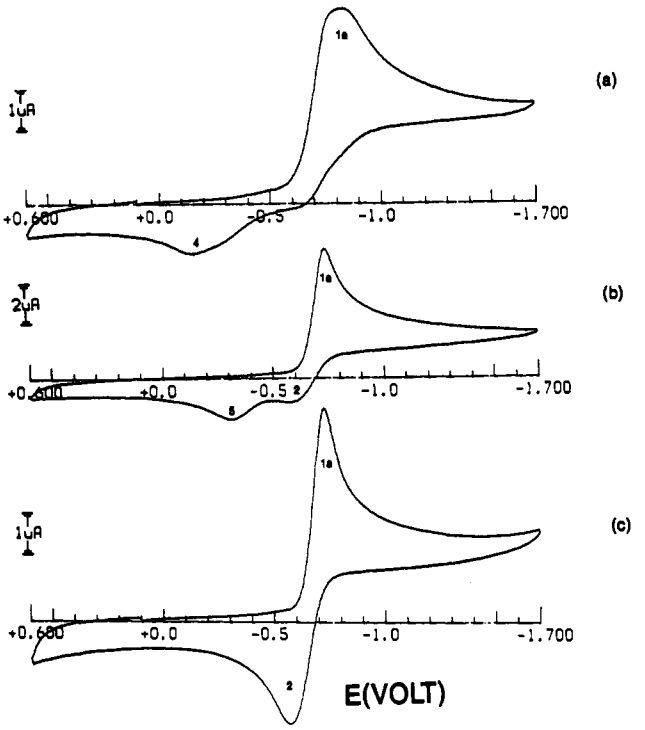

Figure 4. Cyclic voltammograms of a 9.02 × 10^{-4} M solution of [Rh(py)$_4$Cl$_2$]Cl in acetonitrile, 0.17 M TBAP in the presence of (a) no, (b) 0.040 M, and (c) 1.77 M pyridine.

Cyclic voltammograms of [Rh(py)$_4$Cl$_2$]Cl in pyridine, TBAP indicate that if the potential scan is reversed immediately after scanning positive of wave 2, the original reduction wave (wave 1a, Figure 2b) is found. This implies that, following oxidation, [Rh(py)$_4$Cl]$^{2+}$ is generated and rapidly adds one chloride to form the original complex [Rh(py)$_4$Cl$_2$]$^+$, as indicated in Figure 1. Similar results are obtained when cyclic voltammograms of [Rh(py)$_4$Cl$_2$]Cl are run in the presence of excess chloride. When the potential is reversed immediately after scanning positive of wave 3, only the original reduction wave is observed. This was true for scan rates up to 2000 mV/s in both cases.

Figure 4a is the cyclic voltammogram of [Rh(py)$_4$Cl$_2$]Cl in acetonitrile and TBAP, and in this case the reduction process is not as well-defined. It has values of $E_{pc} = -0.82 \pm 0.01$ V vs SCE and $E_{pc} - E_{pc/2} = 120$ mV, at a scan rate of 100 mV/s. If the sample is not vacuum-dried prior to analysis, a broader reduction process is obtained. Under these conditions, the reduction process is a combination of two waves, and the second wave is due to the presence of water. This suggests an ECE mechanism in which chemical reaction with water generates an electroactive species. In agreement, bulk electrolysis data of vacuum-dried samples give values of $n = 1.2$–1.4 in acetonitrile, TBAP, while for undried samples values of n approach 2.0.

Further evidence for an ECE mechanism in the presence of water is found from the observed dependence of the electrochemical behavior on the concentration of water. As the concentration of water is increased, the reduction wave for [Rh(py)$_4$Cl$_2$]$^+$ becomes well-defined and the potential shifts in a positive direction. Hence, in acetonitrile, 0.13 M TBAP in the presence of 14 M H$_2$O, $E_{pc} = -0.54$ V vs SCE and the value of $E_p - E_{p/2}$ is 80 mV at 100 mV/s. No oxidation waves are observed on the return scan in the cyclic voltammogram under these conditions, and bulk electrolysis gives values of n of 2.0 ± 0.1. Hence, the reduction potential and the value of n in the presence of large amounts of water are in agreement with the data previously reported.[22]

If either pyridine (Figure 2b) or another base, such as sodium ethoxide, is added to solutions of [Rh(py)$_4$Cl$_2$]$^+$ in acetonitrile, the reduction wave again becomes a well-defined process. The addition of (TBA)Cl is also found to result in a sharp wave for

the reduction of $[Rh(py)_4Cl_2]^+$ (Figure 2c), due to the hydrophilic nature of this salt.

In the absence of either excess pyridine or chloride (Figure 4a) a reoxidation wave is found at $E_{pa} = -0.16 \pm 0.01$ V (wave 4) and is due to the reduction product formed in the absence of pyridine and chloride. Observation of a distinct product, under these conditions, is in agreement with the loss of a second ligand, as indicated in both paths A and B of Figure 1. In the presence of excess water, wave 4 is not observed and demonstrates this wave is not due to a water reaction product.

Spectroelectrochemical studies demonstrate that, upon reduction of $[Rh(py)_4Cl_2]^+$ in acetonitrile, 0.2 M TBAP at −1.20 V vs SCE, the absorption bands at 255, 260, and 267 nm shift to 256, 262, and 270 nm. At the same time new bands are found at 305 and 369 nm. The absorption band at 410 nm for $[Rh(py)_4(Cl)_2]^+$ is too weak to be monitored with a thin-layer spectroelectrochemical cell, given the solubility limits of the complex.

The spectroelectrochemical data are consistent with metal-centered reduction. This is the case, since only minor shifts were found in the ligand absorption bands at 255, 260, and 267 nm.[24] Ligand-centered reduction for porphyrins[27] and other nitrogen heterocycles[28] typically results in a large change in the ligand electronic absorption bands.

Reoxidation at −0.40 V vs SCE produces no significant spectral changes, while reoxidation at 0.40 V vs SCE results in the original spectrum of $[Rh(py)_4Cl_2]^+$, in agreement with the electrochemical studies. ESR experiments demonstrate that, upon reduction of $[Rh(py)_4Cl_2]^+$ in 0.2 M TBAP, CH_3CN at −1.20 V vs SCE, no signal is detected.

On the basis of the electrochemical, UV–visible spectroelectrochemical, and ESR studies, we tentatively assign the reduction product of $[Rh(py)_4Cl_2]^+$ in acetonitrile, TBAP to be a rhodium(II) dimer, $[Rh(py)_3Cl]_2^{2+}$, as shown in Figure 1. The ESR data and the coulometric data suggest either formation of a rhodium dimer or formation of a rhodium hydride, since only one electron is transferred but no ESR signal is detected. The UV–visible spectrum has similarities to that of the Rh(II) dimer $[Rh_2(CH_3CN)_{10}]^{4+}$, which has electronic absorption bands at 468, 365, and 277 nm.[29] For $[Rh_2(CH_3CN)_{10}]^{4+}$ the absorption band at 468 nm is relatively weak and a similar band would not be observed under our experimental conditions. Hence, in our case, in addition to the pyridine ligand absorption bands (256, 262, and 270 nm), new bands are found at 305 and 369 nm, compared to 277 and 365 nm for $[Rh_2(CH_3CN)_{10}]^{4+}$. However, formation of a rhodium dimer and not a hydride cannot be distinguished from these data alone.

Further evidence for the formation of a rhodium(II) dimer instead of a rhodium hydride is presented in Figure 4b,c. This shows the cyclic voltammograms of $[Rh(py)_4Cl_2]^+$ in CH_3CN, 0.17 M TBAP as a function of pyridine concentration. At intermediate concentrations of pyridine, a new return wave at −0.35 ± 0.01 V (wave 5, Figure 4b) is found. As the concentration of pyridine is increased, wave 5 increases and then decreases to the base line, while wave 2 is found to increase (Figure 4a–c). This suggests successive addition of two pyridines to the reduction product to ultimately form $[Rh(py)_4Cl]^+$ and is consistent with the reduction product being a dimer.

On the basis of the above assignments, wave 4 in Figure 4a, or the reoxidation wave in the absence of excess chloride or pyridine, is due to electron abstraction from $[Rh(py)_3Cl]_2^{2+}$. In agreement with the UV–visible studies, multiple cyclic voltammetric scans demonstrate that this oxidation results in formation of $[Rh(py)_4Cl_2]Cl$. The location of this reoxidation process is close to that found for the rhodium(II) dimer $[(TPP)Rh]_2$, where TPP is the dianion of tetraphenylporphyrin.[5] This species is oxidized at −0.24 V vs SCE in 0.1 M TBAP, benzonitrile.[5] The similarity of the oxidation potentials also provides support for the assignment

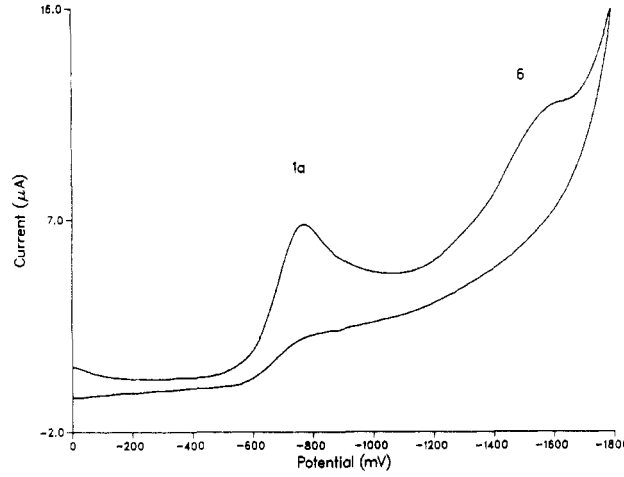

Figure 5. Cyclic voltammogram of a 1.35×10^{-3} M solution of $[Rh(py)_4Cl_2]Cl$ in acetonitrile, 0.16 M TBAP and 0.06 M (TBA)Cl, in the presence of methyl iodide. The approximate ratio of methyl iodide to rhodium is 400:1.

of the one-electron reduction product as a rhodium(II) dimer.

Preliminary Reaction Data for Electrogenerated Species. The rhodium(II) species show reactivity toward a number of different reagents, and these reactions can be monitored by electrochemical techniques. The products of the reactions are unknown and are presently under investigation. An example is the reaction with water, but in addition reactions are also observed with methylene chloride, methyl iodide, and oxygen.

The reactivity of the reduced species is significant when the electrochemical mechanisms previously reported for this complex are evaluated. In aqueous systems $[Rh(py)_4Cl_2]Cl$ is reported to undergo a simple two-electron reduction at a mercury electrode.[21] In a pyridine/water solvent system at a mercury electrode, a two-electron reduction is also reported.[22] However, in the latter case a catalytic mechanism is presented to account for the observation of two overlapping reduction waves.[22] The differences between these studies can probably be attributed to the change in the solvent system. A dependence on the solvent composition was noted[22] but was not rationalized by reaction with water. Our results demonstrate that the presence of water will change the number of electrons transferred from 1 to 2 due to chemical reaction between the electrogenerated rhodium species and water. The products of the reactions of reduced $[Rh(py)_4Cl_2]^+$ with water have been discussed in the literature.[16]

Figure 5 demonstrates the reaction of the rhodium(II) species with methyl iodide. In this figure, the cyclic voltammogram of a 1.35×10^{-3} M solution of $[Rh(py)_4Cl_2]^+$ in 0.16 M TBAP and 0.06 M (TBA)Cl in acetonitrile in the presence of methyl iodide is presented. A new wave at -1.59 ± 0.01 V vs SCE is found (wave 6, Figure 5). Wave 6 is irreversible in the sense that there is no return wave associated with the reduction process. In Figure 5, the approximate molar ratio of methyl iodide to $[Rh(py)_4Cl_2]^+$ is 400:1, and in this case wave 6 is smaller in current than wave 1 and is characterized with an $E_p - E_{p/2}$ of 75 mV. The current for wave 6 suggests that a slow chemical reaction is occurring, involving the reduced rhodium and methyl iodide. It should be added that methyl iodide under exactly the same conditions has no electrochemical processes in the region of interest. In agreement with this assignment, wave 1 remains unchanged but the return process 4 is not observed following scans past wave 6.

The reaction with methyl iodide is of interest, especially when compared to the reactivity of (P)Rh with alkyl halides. In this case, formation of (P)Rh(R)[1-3,6] is observed, which has a very strong metal–carbon bond.[3] The stability of this species limits any following chemistry. For example, (P)Rh(R) is reversibly reduced at potentials near −1.4 V vs SCE.[6,30]

Hence, the electrochemistry of $[Rh(py)_4Cl_2]Cl$ demonstrates formation of rhodium(II) species, with no evidence for formation

(27) Kadish, K. M. *Prog. Inorg. Chem.* **1986**, *34*, 435.
(28) Coombe, V. T.; Heath, G. A.; MacKenzie, A. J.; Yellowlees, L. J. *Inorg. Chem.* **1984**, *23*, 3423.
(29) Dunbar, K. R. *J. Am. Chem. Soc.* **1988**, *110*, 8247.
(30) Anderson, J. E.; Liu, Y. H.; Kadish, K. M. *Inorg. Chem.* **1987**, *26*, 4174.

of lower metal oxidation states in nonaqueous solvents. This is similar to the results obtained for rhodium porphyrins. However, the data for $[Rh(py)_4Cl_2]Cl$ also indicate the electrogenerated species react with several different reagents and that the less rigid ligand set allows observation of new chemical pathways.

Acknowledgment. The ESR experiments were performed by Dr. Y.-H. Liu in the laboratory of Dr. Karl Kadish. Partial support from a BC annual research grant and the loan of rhodium starting material from Johnson Matthey are gratefully acknowledged.

Registry No. TBAP, 1923-70-2; (TBA)(Cl), 1112-67-0; py, 110-86-1; *trans*-$[Rh(py)_4Cl_2]Cl$, 14077-30-6; Rh, 7440-16-6; acetonitrile, 75-05-8; water, 7732-18-5; methyl iodide, 74-88-4.

Contribution from the Department of Chemistry,
Duke University, Durham, North Carolina 27706

Solution Conformations of $CaCl_2$ and $Ca(NO_3)_2$ Complexes of Chiral Tetramethyl 18-Crown-6 Macrocycles: A 1D and 2D ^1H and ^{13}C NMR Investigation

John F. Lewison, Robert G. Ghirardelli, and Richard A. Palmer*

Received March 10, 1989

One- and two-dimensional NMR techniques have been used to investigate the solution structures of (2*S*,6*S*,11*S*,15*S*)-2,6,11,15-tetramethyl-1,4,7,10,13,16-hexaoxacyclooctadecane (I) and (2*R*,3*R*,11*R*,12*R*)-2,3,11,12-tetramethyl-1,4,7,10,13,16-hexaoxacyclooctadecane (II) macrocycle complexes of $CaCl_2$ and $Ca(NO_3)_2$ in $CDCl_3$. Previous chiroptical studies of these and similar crown complexes by circularly polarized luminescence (CPL), total luminescence (TL), and circular dichroism (CD) spectroscopy have shown that the macrocycle asymmetric carbons in these complexes constrain the ring such that the sense of the ring twist in the *S* chiral ring complexes is opposite to that in the *R* chiral ring complexes. These studies have also shown that there is an added chirality element in the di- and trivalent (alkaline earth and lanthanide metal, respectively) nitrate complexes of I and II associated with the twist of the nitrate anions relative to one another as they sterically interact with the ring methyl groups. It has been proposed that channels are created on each face of the macrocycle ring by the axially positioned methyl groups in the solution structures of the I and II complexes and that the planar nitrate anions are constrained to fit in these channels. In this study, we show that the NMR data do indeed support the prominent axial positioning of the methyl groups in the $CaCl_2$ and $Ca(NO_3)_2$ complexes of I and II in solution. Furthermore, the NMR data are consistent with the assertion that the *S* chiral ring (I) twists in an opposite sense to the *R* chiral ring in these complexes. The data for this conformational analysis were obtained by exploiting coupling constant information and the nuclear Overhauser effect, observed by using both one- and two-dimensional NMR techniques.

Introduction

Recently reported chiroptical studies of the solution interactions of chiral crown ether hosts with cations have included the total luminescence (TL), circularly polarized luminescence (CPL), and circular dichroism (CD) spectroscopy of complexes of (2*S*,6*S*,11*S*,15*S*)-2,6,11,15-tetramethyl-1,4,7,10,13,16-hexaoxacyclooctadecane (I) and (2*R*,3*R*,11*R*,12*R*)-2,3,11,12-tetramethyl-1,4,7,10,13,16-hexaoxacyclooctadecane (II)[1-4] (Figure 1).

Of particular interest are the complexes of the alkaline-earth-metal nitrates and of europium nitrate. Analysis of the chiroptical spectra of these complexes has led to the hypothesis of an unusual contribution to the chirality due to the relative orientation of the two associated nitrate anions in the complexes. In both the alkaline-earth and lanthanide complexes spectral and other data indicate that two nitrates are bound (or ion paired) through two oxygens, one nitrate on each "face" of the otherwise flat macrocycle complex. The anions form a two-bladed propeller, the pitch of which is proposed to be influenced by steric interaction with the methyl substituents on the macrocycle ring. The difference in spacing of the methyls around the ring in I and II predicts a different pitch for the dinitrate propeller in the complexes of these isomeric macrocycles and thus a different contribution to the total chirality.

The $n \rightarrow \pi^*$ NO_3^- CD spectra of the alkali-metal ($M^+ = Li^+$, Na^+, K^+, Rb^+) nitrate complexes of I and II have a pseudo-enantiomorphic, mirror image intensity relationship. However, this relationship is not observed between the corresponding complexes of the alkaline earths ($M^{2+} = Mg^{2+}$, Ca^{2+}, Sr^{2+}, Ba^{2+}), where two nitrates are associated. Furthermore, in the crystal structure of the $Ca(NO_3)_2$ complex of II there is a strong indication that the four axially oriented methyl groups in effect create channels across the faces of the macrocycle into which the NO_3^- anions fit. Although no analogous crystal structure data are available for a complex of I, it is clear that its channels, if they exist, would be oriented at ca. 60° to each other, as opposed to almost parallel orientation in II (Figure 2). The influence of these channels is apparently also seen in the CPL spectra of the Eu$(NO_3)_3$ complexes of I and II. (Extensive evidence supports a solution structure for the europium complex essentially identical with that of the alkaline-earth nitrate complexes, with one of the three nitrates not associated.) The fact that the CPL spectra of the europium *chloride* complexes of I and II are virtual mirror images, whereas those of the nitrate show no such relationship, again suggests that it is the nitrate anions which are, together, providing an additional source of chirality (not possible for the spherical chlorides).

This conclusion rests in part on the assumption that other sources of chirality in these complexes are substantially the same in I and II and that, for example, the chiral twist of the macrocycle ring differs only in handedness between the calcium or europium nitrate complexes of I and II. Although this is not an unreasonable assumption, it would be interesting to test it directly by probing the solution conformations of the macrocycle rings more directly. That is the purpose of the study reported here.

Although the numerous investigations of the solution conformations of crown ether macrocycles and their complexes have included a significant number of NMR studies,[5-10] these have all

(1) Metcalf, D. H.; Carter, R. C.; Ghirardelli, R. G.; Palmer, R. A. *Inorg. Chem.* **1988**, *27*, 405.
(2) Metcalf, D. H.; Carter, R. C.; Ghirardelli, R. G.; Palmer, R. A. *Inorg. Chem.* **1986**, *25*, 2175.
(3) Metcalf, D. H.; Ghirardelli, R. G.; Palmer, R. A. *Inorg. Chem.* **1985**, *24*, 634.
(4) Dyer, R. B.; Metcalf, D. H.; Ghirardelli, R. G.; Palmer, R. A.; Holt, E. M. *J. Am. Chem. Soc.* **1986**, *108*, 3621.
(5) Live, D.; Chan, S. I. *J. Am. Chem. Soc.* **1976**, *98*, 3769.
(6) Lockhart, J. C.; Robson, A. C.; Thompson, M. E.; Tyson, P. D.; Wallace, I. H. M. *J. Chem. Soc., Dalton Trans.* **1978**, 611.
(7) Erk, Ç. *Appl. Spectrosc.* **1986**, *40*, 100.
(8) Erk, Ç. *Spectrosc. Lett.* **1987**, *20*, 167.
(9) Kleinpeter, E.; Gäbler, M.; Schroth, W.; Mattinen, J.; Pihlaja, K. *Magn. Reson. Chem.* **1988**, *26*, 387.

0020-1669/89/1328-3909$01.50/0